Evaluation of time sample and span size effects in DES of nominally 2D airfoils beyond stall

A. Garbaruk[1], S. Leicher[2], C. Mockett[3], P. Spalart[4], M. Strelets[1], F. Thiele[3]

[1]New Technologies and Services, St.-Petersburg, Russia
[2]EADS Military Air Systems, Munich, Germany
[3]Technische Universität Berlin & CFD Software GmbH, Germany
[4]Boeing Commercial Airplanes, Seattle, USA

Abstract

A detailed investigation of detached-eddy simulation (DES) applied to the flow around nominally 2D airfoils in deep stall has been conducted. The sensitivity of the flow to a wide range of computational parameters has been assessed. The principal parameters of influence were found to be the length of the time sample computed for Reynolds averaging and the size of the periodic computational domain in the spanwise direction. In contrast, wind tunnel wall effects, the choice of underlying RANS model and the boundary layer transition treatment counted among the parameters for which a low to negligible level of sensitivity was observed. The magnitude of the error introduced by short time samples has been estimated using a statistical analysis technique. This combined with very long time samples (in excess of 2000 non-dimensional units) allows a reliable description of the span size effect independent of the time sample error. The study significantly enhances the body of knowledge concerning this standard validation flow for hybrid RANS-LES methods. The original DES study of Shur et al. (1999), which was conducted for such a flow, is reassessed in light of the new information and its principal conclusions are upheld. The strong level of scatter observed between different experimental sources represents the chief remaining uncertainty.

1   Introduction

The flow over an airfoil in deep stall is one of the most natural applications of detached-eddy simulation (DES) (Spalart et al., 1997, Spalart, 2009). Not surprisingly, precisely such a flow (the NACA0012 airfoil beyond stall) was the first real 3D DES study (Shur et al., 1999), and its success largely ensured the rapid spread of the DES methodology. It has also become a standard test case for the validation of a new DES implementation. However, owing to limited computer power, in this first DES application and in some subsequent studies, simulations were carried out over relatively short time samples and narrow spanwise domains. Furthermore, the experimental data, quoted from the textbook of Hoerner (1965), only involved the mean lift and drag coefficients and no details were given concerning important wind tunnel details such as aspect and blockage ratios. DES was found to perform far better than URANS, which was a very welcome

outcome, however it is now desirable to judge accuracy to better than 10%, more in line with industrial needs. Furthermore, it is necessary to identify and quantify as far as possible the inherent uncertainties in the test case, including the variability seen between equivalent experiments and the sensitivity to computational parameters.

This motivated a further, broader and more computer-intensive, evaluation of DES in predicting stalled airfoil flows, which was carried out within and following the DESider EU project, Haase et al. (2009), and is the subject of this paper. A comprehensive range of parameter studies has been carried out to identify the relative importance of each. The comparison of results also encompasses further levels of analysis, including unsteady force fluctuations and spectra, thereby allowing a deeper evaluation of the predictive capability of DES. In addition to a reassessment of the validity of the conclusions of the original study, this work is therefore also intended to raise the value of the flow as an entry level test case for all hybrid RANS-LES methods.

The paper begins with a description of the flow case and a summary of the available experimental benchmark data, before a concise account of the computational methodologies applied. The analysis of the results begins with a very brief mention of the numerous parameter variations that were found to be of secondary or negligible importance. The bulk of the discussion is thereby dedicated to the two principal sources of test case uncertainty identified, namely the length of the time sample computed for statistical analysis and the extent of the computational domain in the spanwise direction. Following this, the effect of including wind tunnel wall effects in the simulation is assessed. Observe how both the experimental and the numerical studies are aimed at an "ideal" flow, namely the 3D flow over a 2D geometry without any confinement spanwise. Before the conclusion, the implications of the findings upon the interpretation of the original results are discussed.

2 Experimental benchmark data

The experimental benchmark data employed in the original DES study of Shur et al. (1999) is not considered ideal for the reasons outlined in the introduction. This, together with a desire to compare unsteady flow characteristics motivated a search for alternative experimental sources. Data for airfoils at such high angles of attack are unfortunately rather rare, as a consequence of which the inclusion of data for different profiles and Reynolds numbers was necessary. In total, four sets of experimental data were identified, the salient features of which are summarised in Table 1.

The experimental review has two key outcomes. Firstly the effects of Reynolds number, boundary layer tripping and profile thickness (Sheldahl & Klimas, 1981) as well as free-stream turbulence intensity (Swalwell, 2005) were found to be negligible in the range $25° < \alpha < 180°$. The second outcome is highly frustrating for the purposes of CFD validation: A tremendous degree of scatter is apparent between facilities, e.g. 12% for C_l at $\alpha = 60°$. In the absence of any information

about the relative fidelity of the experiments, no strong conclusions can be drawn from comparison of mean force coefficients between DES results and experimental data.

Table 1 *Summary of relevant experimental data for symmetric NACA profiles. The mean and standard deviation values quoted are for $\alpha = 60°$.*

Reference	Profile	$Re_c(\times 10^5)$	α_{max}	$\overline{C}_l$	$\overline{C}_d$	$\sigma[C_l]$	$\sigma[C_d]$	Spec	$\overline{C}_p(x)$
Hoerner (1965)	0012	1.0	180°	0.92	1.65	—	—	—	—
Sheldahl & Klimas (1981)	0021	3.6	180°	0.875	1.470	—	—	—	—
Swalwell et al. (2004)	0021	2.7	90°	0.93	1.55	0.104	0.151	Yes	Yes
Raghunathan et al. (1988)	0021	2.6	90°	0.82	—	—	—	—	—

Re_c Reynolds number based on chord length and free-stream velocity, α_{max} maximum angle of attack measured, $\overline{C}_l$, $\overline{C}_d$ time-averaged lift & drag coefficient at $\alpha = 60°$, $\sigma[C_l], \sigma[C_d]$ standard deviation of lift and drag coefficient, *Spec* force spectra available? $\overline{C}_p(x)$ surface pressure distribution available?

3 Computational methodology

Table 1 reveals only one experiment with time-resolved data, namely that of Swalwell et al. (2004). For this reason, the test case was adopted within later studies, beginning with the EU DESider project (Haase et al., 2009). The corresponding NACA0021 airfoil at $Re_c = 2.7 \times 10^5$ was simulated and the decision was made to focus upon a single angle of attack, namely $\alpha = 60°$. All reported results were obtained from fully-turbulent computations and the force coefficients were integrated over a single spanwise position (as in the experiment). Results computed by three partners are drawn upon, referred to by the following acronyms: EADS Military Air Systems (EADS), New Technologies and Services (NTS) and Technische Universität Berlin (TUB). The NTS and TUB simulations assumed infinite far-field conditions and periodicity in the spanwise (z) direction. The EADS computation by contrast included free-slip wall boundary conditions in the vertical and lateral directions, at locations corresponding to the wind tunnel geometry. In all cases a sufficient number of time steps were excluded before Reynolds averaging to remove initial transient. A summary of all computations is given in Table 2.

The computational grids employed are depicted in Fig. 1. The structured, O-topology grid generated by NTS was used in the simulations of NTS and TUB. EADS generated their own unstructured hybrid mesh in which the boundary layer region is resolved using prismatic cells. In both cases the grids have been uniformly extruded in the spanwise direction.

Table 2 *Summary of simulations conducted.*

Partner	Model	L_z/c	Δ_z/c	Δ_{xy}/c	N_{xyz}	$\Delta t \times |U_\infty|/c$	$T_{avg} \times |U_\infty|/c$
EADS	SA-DES	7.2	0.025	0.014	19.2M	0.07	430
NTS	SA-DES	1.0	0.03	0.037	0.5M	0.03	2100
		1.4			0.7M		2100
		2.0			1.0M		2000
		2.8			1.4M		2000
		4.0			2.0M		2500
TUB	SALSA-DES	1.0	0.03	0.037	0.5M	0.025	1000
	LLR-DES	1.0			0.5M		1200
	CEASM-DES	1.0			0.5M		1600
		3.24			1.6M		700
	SA-DES	4.0			2.0M	0.03	2300

SA Spalart & Allmaras (1992) model, *SALSA* strain-adaptive linear SA model of Rung et al. (2003), *LLR* local linear realisable model of Rung & Thiele (1996), *CEASM* compact explicit algebraic stress model of Lübcke (2001), L_z spanwise domain size, Δ_z spanwise grid cell size, Δ_{xy} typical x/y cell size in focus region, N_{xyz} number of grid cells, Δt time step size, T_{avg} physical time sample for Reynolds averaging.
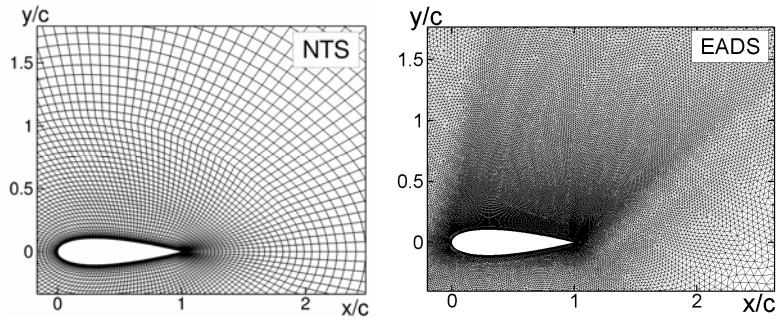
Fig. 1 The computational grids employed (the spanwise-normal plane is shown).

Due to space constraints only a summary description of the flow solvers will be given. EADS employed the unstructured DLR Tau code (Schwamborn et al., 1998) whereas NTS (Strelets, 2001) and TUB (Xue, 1998) used in-house multi-block structured codes. The convective terms in Tau are approximated using a central differencing scheme with matrix dissipation of the Jameson type for stabilisation. The NTS and TUB solvers both employ a hybrid convection scheme conceived for DES (Travin et al., 2000), whereby the localised blending is between 4th order central and 5th order upwind schemes in the NTS code and between 2nd order central and upwind-biased TVD schemes in the TUB code.

4 Presentation and discussion of results

4.1 Summary of related findings

The detailed discussion of the results in the following sections concern the parameters to which the flow proved highly sensitive. However, a great deal of other parameter variation studies have been carried out, the results of which have in many cases remained unpublished because of the weak sensitivity found. It is nonetheless important to summarise these findings.

A minor sensitivity of the integral forces and negligible sensitivity of the spectra to the underlying RANS model has been observed in studies by TUB (Mockett, 2009) and NTS (Haase et al., 2009). In comprehensive studies by NTS, the sensitivity to the boundary layer transition treatment, mild variations of the time step size and the overall grid resolution as well as the resolution of the leading edge curvature and the time step size has been found to be negligible. Many of these results indicate the weak overall importance of the attached boundary layer prediction, and can be related to the weak effects of Reynolds number and free stream turbulence reported in the experiments.

4.2 Effect of time sample

The accuracy of statistical estimates naturally depends upon the sample length available. Usual practice in such unsteady simulations is to compute "long" samples and to assume that the statistical error is negligible. What time sample length is considered "long" is unfortunately often a strong function of the computational resources and time available. In more thorough analyses, e.g. Haase et al. (2009), running averages are inspected to give a qualitative feel for the level of variability present in the statistics. However, even after long averaging durations these trends can still give rise to surprises in the form of strong and sudden drift in the mean value. Most importantly, no quantitative error estimate is obtained from this technique. The time signals of the integral forces from this flow case unfortunately exhibit very long wavelength random modulation and a multi-modal character, as seen in both experiment (Swalwell et al., 2004) and DES (Haase et al., 2009, Mockett, 2009). As a result it is expected that very long time samples are necessary.

To obtain quantitative estimates of the statistical error arising due to the finite time sample available, a technique developed recently at TUB is applied. A full description of this technique is outside the scope of this paper and would indeed necessitate a dedicated paper. The method employs a standard definition of the random error occurring in statistically stationary data (Bendat & Piersol, 1986), which is computed by subdividing the available data into windows. Employing analytically-derived relationships for bandwidth-limited white noise, case-specific expressions of the statistical error as a function of sample size, T_{avg}, are returned. The sole input is the time series in question and no further user parameters are required. The following expressions have been derived for the normalised error, ε,

in the estimated mean, $\hat{\mu}$, and standard deviation, $\hat{\sigma}$, of the lift and drag coefficient:

$$\varepsilon\left[\hat{\mu}_{C_l}\right]=\frac{1.83}{\sqrt{T_{avg}}}\left(\frac{\sigma_{C_l}}{\mu_{C_l}}\right)\times100\% , \quad \varepsilon\left[\hat{\mu}_{C_d}\right]=\frac{2.36}{\sqrt{T_{avg}}}\left(\frac{\sigma_{C_d}}{\mu_{C_d}}\right)\times100\% , \tag{1}$$

$$\varepsilon\left[\hat{\sigma}_{C_l}\right]=\frac{1.29}{\sqrt{T_{avg}}}\times100\% , \quad \varepsilon\left[\hat{\sigma}_{C_d}\right]=\frac{1.67}{\sqrt{T_{avg}}}\times100\% ,$$

where μ_x and σ_x are the mean and standard deviation of the quantity x computed from the entire signal, respectively. T_{avg} is given in dimensionless quantities, as specified in Table 2. These expressions, the constants for which are computed from the experimental time series (of length $T = 8860$ c/U_∞ and derived from a single section), have been found to hold for the DES data of varying span size when the respective computed values of μ_x and σ_x are used. The error trends for the wide domain DES furthermore agreed excellently with those from the experiment. Notably, the difference in the error trend between sectional force data and that integrated over the entire span was seen to be negligible.

The expressions of Eq. (1) therefore allow statistical error bars to be placed on the mean and standard deviations of the DES forces, which is indeed done in the following section. Such analysis furthermore enables the engineer to estimate the number of time steps required to achieve the desired level of statistical accuracy for a particular flow case. For the DES with $L_z = 4c$ for example, Eq. (1) stipulates that a time sample of roughly 530 c/U_∞ is required to achieve 1% accuracy in the mean forces.

4.3   Span-size effects

The spanwise distance between the periodic boundaries to the computational domain has been varied between $L_z = 1c$ and $4c$ in the calculations of NTS and TUB, allowing the influence of this user parameter to be studied. Figures 2 and 3 draw upon all DES results employing a periodic spanwise domain and all applicable experimental data to provide an overview. The magnitude of the statistical error obtained from Eq. (1) is portrayed in the figures by error brackets.

The effect of a narrow span size is to increase all quantities depicted. The effect is indeed pronounced, far outweighing the statistical error and the model/code dependency. When long time samples are computed, L_z hence constitutes the most influential source of error. It is to be expected that this finding would apply to nominally 2D bluff bodies in general. Furthermore, since the ratio σ/μ increases, it can be seen from (1) that the statistical error of the mean forces is greater for shorter L_z and a given T_{avg}. This effect is so strong that $L_z = 4c$ becomes computationally less expensive than $L_z = 1c$ to a desired statistical accuracy.

The plots of Figs. 2 and 3 suggest that the L_z influence becomes marginal at values of around $4c$ for this test case, although further computations at still larger L_z values would strictly be required to demonstrate this[1]. An indication that the

---

[1] With exception of the $L_z = 1c$ data, the results appear to scale according to L_z^{-2}.

required L_z is strongly case-specific is given by comparison with the results of Guenot (2004) for the lower $\alpha = 45°$ case. In that case, the L_z effect was seen to settle at lower values of $L_z \approx 2c$. It is believed that the wider wake is responsible for the larger L_z required for our $\alpha = 60°$ case.

The mean surface pressure coefficient, C_p, plotted in Fig. 4, corroborates the trend shown by Fig. 2 and shows that the L_z effect is manifested in a strong variation of the base pressure on the downstream (upper) surface of the airfoil. The paradox that the agreement with experiment degrades with increasing L_z was initially a source of concern. However, the observation of a strong scatter between the experiments (particularly visible in Fig. 2) reduces this. Furthermore, the conclusion to be reached from Fig. 2 is that increasing L_z brings the mean C_l inside the experimental range and in excellent agreement with the Sheldahl & Klimas data. For the mean C_d however, the agreement is less positive. This could in part be because the C_d value from the Raghunathan et al. experiment, expected to be low, is unknown.
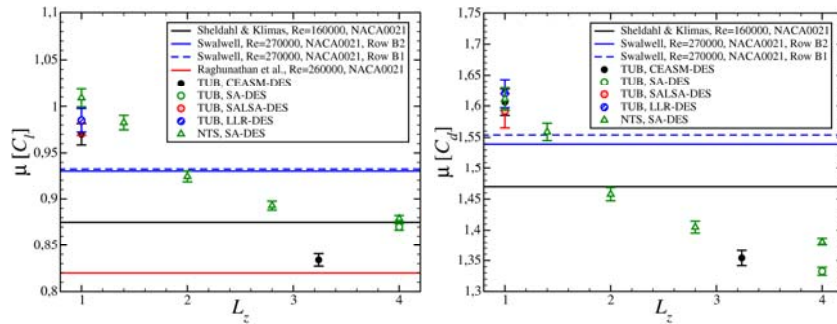

Fig. 2 Trends of mean lift and drag coefficient against L_z for the NACA0021 at $\alpha = 60°$ and Re = 270000 (unless otherwise stated).
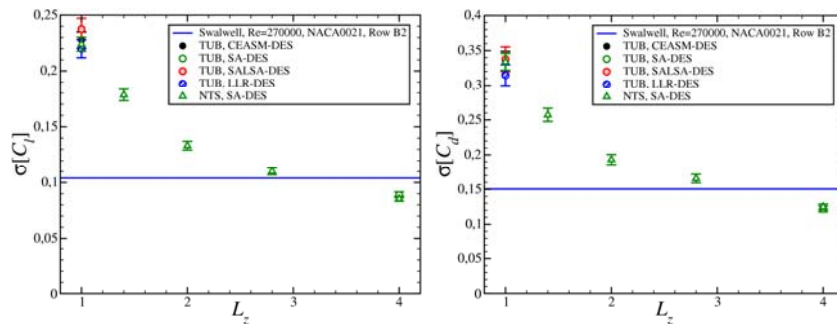

Fig. 3 Trend of standard deviation of the lift and drag coefficients with L_z for the NACA0021 at $\alpha = 60°$ and Re = 270000.

Despite the poor agreement of the mean quantities with Swalwell's experimental data, the story for the unsteady quantities is very different: A strong improvement in the standard deviation of the integral forces is achieved at longer L_z values (Fig. 3). More detail is offered by the power spectral density (PSD) of C_l, plotted in Fig. 5. Particularly regarding the lowest frequencies, the agreement of the broadband energy is strongly improved at $L_z = 4c$. The sharp spectral peak at St $\approx$ 0.2 represents the vortex shedding frequency and the strong disagreement in its energy is troublesome, however. Although not clearly visible in the plot of Fig. 5, the computed peak energy ranges between 30% (TUB) and 50% (NTS) of the experimental value.
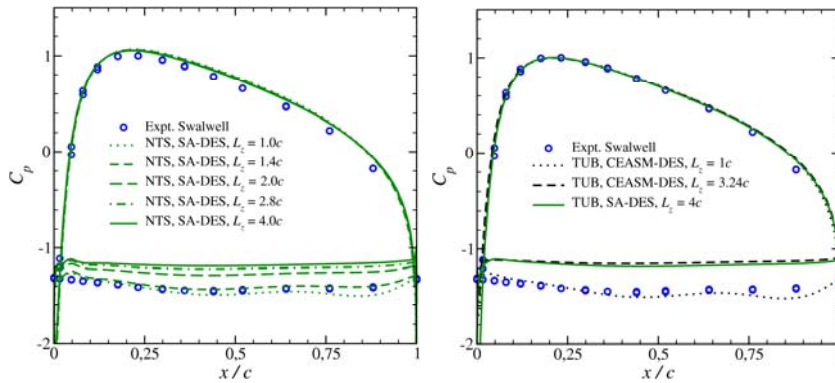
Fig. 4 The effect of L_z on the mean C_p distribution. Comparison of NTS (*left*) and TUB DES (*right*) with experiment.
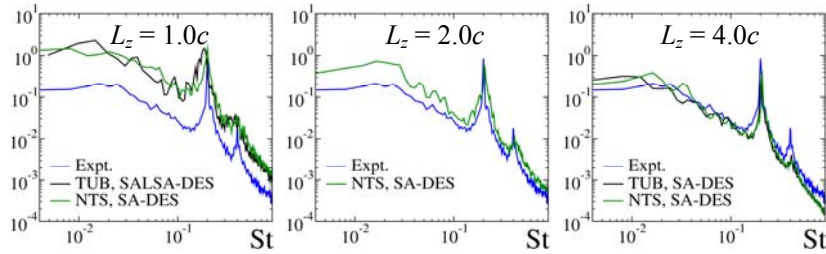

Fig. 5 PSD of C_l comparing NTS and TUB DES for varying L_z with experiment.

A natural statistical quantity to examine in such an investigation is the two-point correlation of velocity in the spanwise direction, $R_{ii}(z)$, where i represents the u, v and w components. These are plotted in Fig. 6 at four probe positions in the near wake for TUB computations at $L_z = 1c$ and $L_z = 4c$. For the u and v components, the correlations settle to lower values in the wider domain, however they clearly remain above zero. Such long spanwise correlation lengths naturally arise due to the strong spanwise coherence of the large-scale vortex shedding. For

the w component a different behaviour is seen: In the narrow domain the correlation consistently reaches a negative value, implying an anti-phase behaviour. For the longer domain however, the w correlation settles around zero. It is therefore suggested that $R_{ww}(z)$ could provide a generic test for sufficient span size in practice. This would however require more testing to confirm.
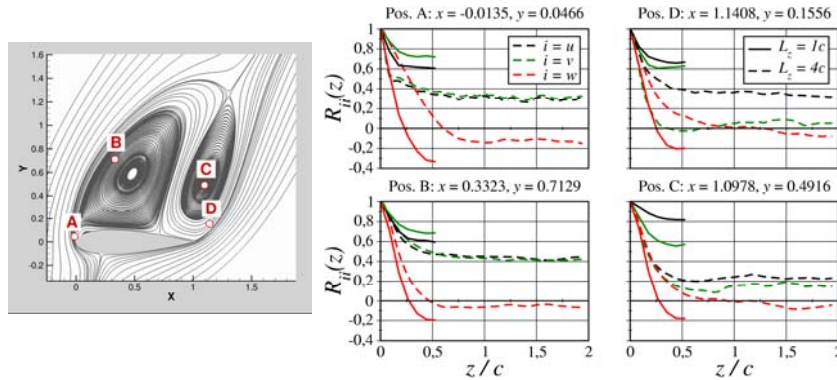
Fig. 6 Two-point spanwise correlations of u, v and w compared for $L_z = 1c$ (TUB CEASM-DES) and $L_z = 4c$ (TUB SA-DES) at various probe locations.

Finally, further insight into the span size effect can be obtained from instantaneous visualisations of the resolved vortex structures (Fig. 7). The streamwise rib vortices and spanwise von Kármán vortices maintain a high degree of orthogonality in the narrow spanwise domain. In contrast, these exhibit less orthogonality with spanwise dislocations and higher degrees of slant apparent in the wider domain.
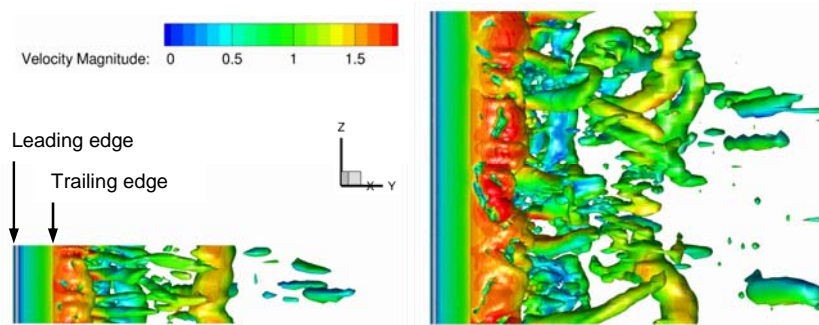
Fig. 7 Instantaneous snapshots of resolved vortical structures compared between $L_z = 1c$ (TUB CEASM-DES) and $L_z = 4c$ (TUB SA-DES) calculations. Isosurfaces of $\lambda_2 = -4$ (Jeong & Hussain, 1995) shaded with velocity magnitude, view from below (facing the trailing edge).

4.4   Effect of wind tunnel walls

It was suspected that the surrounding wind tunnel walls, neglected in the spanwise-periodic computations, may contribute to the discrepancy with the Swalwell experiments. This was the motivation for the EADS simulation including the wind tunnel walls with free-slip boundary conditions. The mean surface C_p and PSD of C_l plotted in Fig. 8 indicate a negligible impact of the tunnel walls. The time-averaged force coefficients give a similar message: The C_l = 0.89 ± 0.01 and C_d = 1.43 ± 0.02 from the computation with wind tunnel walls do not differ significantly from the NTS periodic computation (C_l = 0.88 ± 0.003 and C_d = 1.38 ± 0.006). Although the comparison is unfortunately not direct (employing different L_z, solvers, grid resolution and time step), the experience of various related investigations implies that these factors have a negligible influence for this test case.
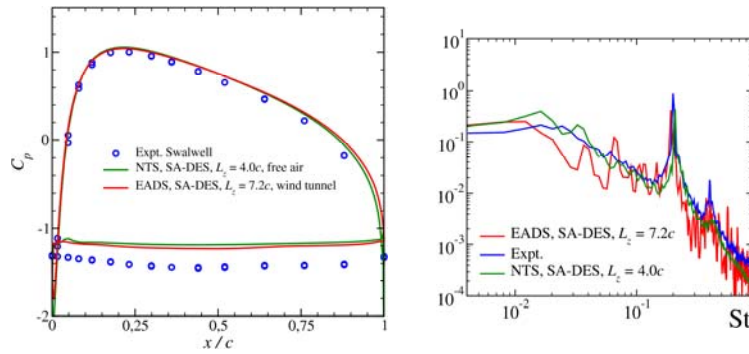
Fig. 8 Comparison of mean surface C_p (*left*) and PSD of C_l (*right*) between the spanwise-periodic NTS computation ($L_z = 4c$) and the EADS computation with tunnel walls ($L_z = 7.2c$) and with experiment.

5   The original DES study revisited

In light of all that has since been learned about this test case, it is interesting to revisit the pioneering DES study of Shur et al. (1999): To what extent are the original conclusions regarding the DES predictive capability for such flows still valid? It is now clear that the employed span size of one chord significantly distorts the mean force coefficients. Likewise, the simulated time samples (quoted in the range $100 < T_{avg} \times |U_\infty| / c < 200$) can be expected to add an appreciable error bracket to the statistical quantities. How can we therefore interpret the high level of agreement that was seen with the experimental data of Hoerner (1965)?

   A single data point from the Shur et al. results, namely at the $\alpha = 60°$ value that formed the focus of subsequent investigations, has been analysed in Table 3. Assuming the same statistical error trend as that determined for the NACA0021

profile, corresponding error bands have been added to the original mean force coefficients. To estimate the influence of the narrow span size, the original values have furthermore been re-scaled using the difference in force coefficient observed between $L_z = 1c$ and $L_z = 4c$ for the NACA0021. Although the original results agreed well with the experimental values quoted by Hoerner, the values re-scaled to $L_z = 4c$ agree excellently with the alternative experimental data provided by Sheldahl & Klimas. The message is therefore that the latest findings serve to reinforce rather than undermine the original conclusions of Shur et al.

Table 3 *Comparison of the original and span size rescaled NACA0012 DES results of Shur et al. (1999) with the Sheldahl & Klimas (1981) (S&K) experimental data.*

Case:	Mean C_L:	C_L deviation rel. to S&K	Mean C_D:	C_D deviation rel. to S&K
DES, Shur et al. (1999), Re = 100000, $L_z = 1c$	1.00 ± 0.02	+14 %	1.69 ± 0.04	+15 %
Above result rescaled to $L_z = 4c$	0.87 ± 0.02	–0.6 %	1.46 ± 0.03	–0.7 %
Exp, Sheldahl & Klimas (1981), Re = 160000	0.875	—	1.470	—

6   Conclusions

This study has drawn upon a large body of simulations involving numerous parameter variations and has shed considerable light on the dominant sources of uncertainty for DES of nominally 2D airfoils in deep stall. Two key factors have been found to affect the results, namely the length of the time sample simulated and the spanwise domain size. Thanks to the statistical error analysis method, the former effect could be quantified. It emerges that around 530 non-dimensional time units must be computed to achieve at least 1% accuracy in mean lift and drag for $L_z = 4c$. The strong influence that a narrow span size has on the mean and fluctuating forces has been documented. The computation of very long time samples has furthermore served to separate the span size influence from the statistical error. A key result of this study concerns the interaction of these dominant parameters of influence: A further effect of a narrow domain size is a strong increase in the time sample requirements to reach the same level of statistical accuracy in the mean force coefficients. For $L_z = 1c$, time samples in the region of 2400 non-dimensional units are required to achieve the same 1% accuracy in the mean forces. So strong is the effect that once initial transient has been removed, it is in fact computationally *less* expensive to simulate the longer spanwise domain size of $L_z = 4c$ when the mean forces are of primary interest[2].

Standing in contrast to the time sample and span size, the variation in the results due to the choice of underlying RANS model, conducted primarily for L_z =

---

[2] Note that this does not apply to the standard deviations, the statistical error upon which is unaffected by the span size (Eq. (1)).

$1c$, is weak and of a similar magnitude to the statistical error. This is in accordance with the experimental observation that the flow is robust to variations in the Reynolds number and the free stream turbulence intensity. This weak model sensitivity for DES when applied to such flows represents a key advantage over URANS (for which significant model sensitivity has been established). A further encouraging result has been the demonstration of excellent agreement between the NTS and TUB computations in a direct comparison of the different codes. Finally, an indication has furthermore been given that the influence of wind tunnel walls is also weak, although a more direct comparison would be desirable.

The best agreement of the mean forces is with the Sheldahl & Klimas data and the comparison of force spectra with the data of Swalwell is encouraging in many respects. However, a fundamental obstacle remains due to the strong experimental scatter. A more detailed and critical review of the experiments with the goal of reducing this would hence be a valuable future contribution. As things stand, the primary suitability of the flow case is for the cross-verification of CFD methods.

Finally, rather than challenging the conclusions of the pioneering DES study of Shur et al. (1999), which established the significant advantages of DES over URANS, the current work has served to reinforce these.

References

Bendat JS, Piersol AG (1986) Random data, analysis and measurement procedures. John Wiley & Sons, Inc., New York Chichester Brisbane Toronto Singapore

Guenot D (2004) Simulation des effets instationnaires à grande échelle dans les écoulements décollés. Ph.D. thesis, SUPAERO

Haase W, Braza M, Revell A (eds) (2009) DESider – A European effort on hybrid RANS-LES modelling. Notes Numer Fluid Mech Multidiscip Design 103. Springer, Berlin Heidelberg New York

Hoerner S (1965) Fluid-dynamic drag. Hoerner Fluid Dynamics, New Jersey

Jeong J, Hussain F (1995) On the identification of a vortex. J Fluid Mech 285:69–94

Lübcke H (2001) Entwicklung expliziter Darstellungen zweiter statistischer Momente zur numerischen Simulation turbulenter Strömungen. Ph.D thesis, Technische Universität Berlin

Mockett C (2009) A comprehensive study of detached-eddy simulation. Ph.D. thesis, Technische Universität Berlin

Raghunathan S, Harrison JR, Hawkins BD (1988) Thick airfoil at low Reynolds number and high incedence. J Aircr 25(7):669–671

Rung T, Thiele F (1996) Computational modelling of complex boundary-layer flows. In: Proc 9th Int Symp Transp Phenom Therm-Fluid Eng, Singapore

Rung T, Bunge U, Schatz M, Thiele F (2003) Restatement of the Spalart–Allmaras eddy-viscosity model in strain-adaptive formulation. AIAA J 41(7):1396–1399

Schwamborn D, Gerhold T, Hannemann V (1998) On the validation of the DLR Tau code. In: Nitsche W, Heinamann HJ, Hilbig R (eds) New Results Numer Exp Fluid Mech II. Springer, Berlin Heidelberg New York

Sheldahl RE, Klimas PC (1981) Aerodynamic characteristics of seven symmetrical airfoil sections through 180-degree angle of attack for use in aerodynamic analysis of vertical axis wind turbines. Sandia National Laboratories SAND80-2114

Shur M, Spalart PR, Strelets M, Travin A (1999) Detached-eddy simulation of an airfoil at high angle of attack. In: Rodi W, Laurence D (eds) Eng Turbul Model Exp 4. Elsevier, Amsterdam, pp 669–678

Spalart PR (2009) Detached-eddy simulation. Annu Rev Fluid Mech 41:181–202

Spalart PR, Allmaras SR (1992) A one-equation turbulence model for aerodynamic flows. In: Proc 30th AIAA Aerosp Sci Meet Exhib, Reno

Spalart PR, Jou W, Strelets M, Allmaras SR (1997) Comments on the feasibility of LES for wings, and on a hybrid RANS/LES approach. Adv DNS/LES 1

Strelets M (2001) Detached eddy simulation of massively separated flows. In: Proc 30th AIAA Aerosp Sci Meet Exhib, Reno

Swalwell K (2005) The effect of turbulence on stall of horizontal axis wind turbines. Ph.D thesis, Monash University

Swalwell K, Sheridan J, Melbourne W (2004) Frequency analysis of surface pressure on an airfoil after stall. In: Proc 21st AIAA Appl Aerodyn Conf

Travin A, Shur M, Strelets M, Spalart PR (2000) Physical and numerical upgrades in the detached-eddy simulation of complex turbulent flows. In: Friedrich R, Rodi W (eds) Advances in LES of Complex Flows, Kluwer Acad., New York

Xue L (1998) Entwicklung eines effizienten parallelen Lösungsalgorithmus zur dreidimensionalen Simulation komplexer turbulenter Strömungen. Ph.D thesis, Technische Universität Berlin